https://doi.org/10.5194/egusphere-2023-710
Preprint. Discussion started: 15 May 2023

Day-night differences in $\delta^{18}O$ and *d*-excess of convective rainfall in the Rio Claro station, inland tropics of Brazil

Vinicius dos Santos[1], Didier Gastmans[1], Ana María Durán-Quesada[2], Ricardo Sánchez-Murillo[3], Kazimierz Rozanski[4], Oliver Kracht[5] and Demilson de Assis Quintão[6].

[1]São Paulo State University (UNESP), Environmental Studies Center. Av. 24ABased, 1515, Bela Vista, 13.506-900, Rio Claro, São Paulo, Brazil. vinicius.santos16@unesp.br; didier.gastmans@unesp.br

[2]Escuela de Física & Centro de Investigación en Contaminación Ambiental & Centro de Investigaciones Geofísicas, Universidad de Costa Rica, San José 11501, Costa Rica. ana.duranquesada@ucr.ac.cr

[3]University of Texas at Arlington, Department of Earth and Environmental Sciences, 500 Yates Street, Arlington, Texas 76019, USA. ricardo.sanchezmurrillo@uta.edu

[4] Faculty of Physics and Applied Computer Science, AGH University of Science and Technology, al. Mickiewicza 30, 30-059 Krakow, Poland. rozanski@agh.edu.pl

[5]International Atomic Energy Agency, Isotope Hydrology Section, Vienna International Centre, P. O. Box 100, 1400 Vienna, Austria. O.Kracht@iaea.org

[6]São Paulo State University (UNESP), IPMet/Science College, Est. Mun. José Sandrin IPMET, S/N, 17.048-699, Bauru, São Paulo, Brazil. demilson.quintao@unesp.br

Correspondence to: Didier Gastmans (didier.gastmans@unesp.br)

Abstract. The tropical central-southern part of Brazil (CSB) is characterized by strong convective systems bringing generous water supply for agro-industrial activities but also pose flood risks for large cities. Here, we present high-frequency (5-10 minutes) rainfall isotopic compositions to better understand those systems, with a total of 90 intra-event samples collected during the period 2019-2021. Convective activity and moisture transport modulate the seasonal rainwater isotopic composition with low $\delta^{18}O$ values during summer and high during autumn and spring. In summer, both regional and local factors contribute to the observed depletion in heavy isotope contents of rainfall, with strong, continuous rainout along the trajectories of moisture-laden air masses arriving at the rainfall collection site from the Amazon basin, and diurnal convective activity of the local atmosphere, respectively. This activity generates convective clouds with distinct features (cloud depth and cloud base height) and induces differences in atmospheric conditions below the cloud base level (relative humidity and rainfall rates) modifying isotopic characteristics of rainfall and revealing novel perspective on day-night contrast in $\delta^{18}O$ and *d*-excess values. During daytime, enhanced sub-cloud effects lead to high $\delta^{18}O$ and low *d*-excess while continuous regional rainout during night-time results in low $\delta^{18}O$ and high *d*-excess values of local rainfall. Our results offer a new framework of key drivers controlling the isotopic variability of rainfall in tropical South America that must be considered in future studies of convective systems across the tropics.

https://doi.org/10.5194/egusphere-2023-710
Preprint. Discussion started: 15 May 2023

1 Introduction

The central-southern part of Brazil (CSB) is the main contributor to the Brazilian economy, with agriculture and industry as leading activities (Zilli et al., 2017). These sectors strongly depend on rainfall seasonality for irrigation and hydropower supply (Luiz Silva et al., 2019). Suggested changes in frequency of heavy and extreme rainfall events in future climate scenarios (Marengo et al., 2020; Donat et al., 2013; IPCC, 2021) may represent a serious threat to regional economic activities and electricity generation. Similarly, climate projections also suggest that enhancement of heavy rainfall events will aggravate the occurrence of both floods and landslides across vulnerable areas (Marengo et al., 2020), whose total cost has risen to US$ 41.7 billion in the past 50 years (Marengo et al., 2020; World Meteorological Organization, 2019).

Extreme rainfall events are related to the convective systems (CS), characterized by strong vertical development in the form of *cumulus-nimbus* and *cumulus congestus* (convective clouds) and low-level convergence (stratiform clouds) (Siqueira et al., 2005; Machado and Rossow, 1993; Zilli et al., 2017), commonly refer to as convective and stratiform rainfall, that account for 45% and 46% of the total rainfall in South America, respectively (Romatschke and Houze, 2013). These rainfall types have recently been postulated as a major driver explaining variations in stable isotope composition of precipitation across the tropics (Zwart et al., 2018; Sánchez-Murillo et al., 2019; Sun et al., 2019; Han et al., 2021; Aggarwal et al., 2016). Specifically, the role of tropical convection in formation of the isotopic composition of rainfall has been discussed in the context of so-called amount effect (heavy isotope contents of tropical precipitation decrease as the amount of local precipitation increases) (Dansgaard, 1964; Hu et al., 2018; Kurita, 2013a; Rozanski et al., 1993; Winnick et al., 2014; Tharammal, T., G. Bala, 2017).

Previous studies used satellite retrievals of atmospheric water vapor isotopic composition to better understand convective processes in other regions (Lawrence et al., 2004; Worden et al., 2007; Kurita, 2013b). They showed the links between the structure and depth of convective systems; and variations in the isotopic composition of local vapor, being strongly depleted in ^{18}O with for deep convection systems. Consequently, similar relations were observed for local rainfall, confirming the important role of convection systems in reducing heavy isotope contents of precipitation in the tropics (Lekshmy et al., 2014; Vuille et al., 2003; dos Santos et al., 2022). Despite these advances, to date only few studies have examined the rainfall isotopic composition in the light of diurnal variations in convective activity of tropical atmosphere (Munksgaard et al., 2020; Moerman et al., 2013).

Diurnal variations in heating of the surface intensify convection processes, generating short-lived events that can occur in consecutive days across the tropics (Romatschke and Houze, 2013, 2010). These events are characterized by a diurnal cycle and notable differences in: (i) rainfall intensity, (ii) vertical extent of convective cores between deep and shallow convection, and (iii) life cycle of these events in Mesoscale Convective Systems (MCSs) (Schumacher and Houze, 2003; Romatschke and Houze, 2013, 2010). Convective events account for a significant proportion of annual rainfall and are linked with extreme events over the land, with most intense events occurring in the afternoon (Schumacher and Houze, 2003; Kurita, 2013a; Wang

https://doi.org/10.5194/egusphere-2023-710
Preprint. Discussion started: 15 May 2023

and Tang, 2020). High-frequency rainfall sampling strategies during the occurrence of convective events are needed to capture the diurnal heating cycle and associated variations in the isotopic signatures of convective rainfall.

High-frequency rainfall sampling and analyses of stable isotope ratios has been used to better understand the evolution of large atmospheric systems such as tropical cyclones and typhoons (Sun et al., 2022; Sánchez-Murillo et al., 2019; Han et al., 2021) and local evaporation effects (Graf et al., 2019; Aemisegger et al., 2015b; Lee and Fung, 2008). This high-resolution isotope information provided a better insight into the development of weather systems and cloud dynamics, both responsible for changes in the rain type, intensity, and inherent isotope variability during rainfall events (Coplen et al., 2008; Muller et al., 2015; Celle-Jeanton et al., 2004). However, high-frequency isotope sampling of rainfall has been limited across the tropics, despite convective activity being significant in this region.

Using high-frequency rainfall sampling strategy we focus here on processes controlling isotopic composition of rainwater on diurnal time scale, which are of local (below-cloud evaporation and exchange processes, vertical structure of rainfall, cloud top over sampling site, and others) and regional (moisture origin/transport, regional atmospheric circulation, and convective activity). Evolution of convection systems on the diurnal cycle is used here only to characterize the clouds during day and night situations. We combine high-frequency rainfall sampling with ground-based observational data (Micro Rain Radar, and automatic weather station) with satellite imagery (GOES-16), ERA-5 reanalysis products and HYSPLIT trajectories to study the day-night differences in isotopic composition of convective rainfall collected over the inland tropics of Brazil.

2 Data and Methods

2.1 Sampling site and atmospheric systems

The rainfall sampling site was localized in Rio Claro city, São Paulo State (Fig. 1a). The station (-22.39°S, -47.54°W, 670 m.a.s.l) belongs to Global Network of Isotopes in Precipitation network (GNIP) and is influenced by atmospheric systems responsible for rainfall variations and seasonality linked to the regional atmospheric circulations of CSB region. The rainfall seasonality over CSB is associated with: (i) Frontal Systems (FS), represented mainly by Cold Fronts from southern South America (SA) acting all the year, and (ii) the South Atlantic Convergence Zone (SACZ) during austral summer (December to March) (Kodama, 1992; Garreaud, 2000) (Fig. 1b). These synoptic features are mostly responsible for the development of CS (Romatschke and Houze, 2013; Siqueira et al., 2005; Machado and Rossow, 1993) (Fig. 1c), and were captured during their passage over the Rio Claro station..

2.2 Rainfall sampling and isotope analyses

Rainwater was manually collected with a passive collector at 5-10 minutes intervals, from September 2019 to February 2021, except for April, July, and August 2020, when no rainfall was observed in the study area (Fig. 2). Due to the difficulties of

https://doi.org/10.5194/egusphere-2023-710
Preprint. Discussion started: 15 May 2023

manual sampling and complexity in forecast rainfall occurrences for one point, rainfall events were collected randomly during the monitoring period. Rainfall samples (n = 90) were immediately transferred and stored in 20 mL HDPE bottles with sealed caps. Air bubbles were avoided to prevent potential isotopic exchange with the headspace and fractionation.

Rainfall samples were analysed for stable isotope composition using Off-Axis Integrated Cavity Output Spectroscopy (Los Gatos Research Inc.) at the Hydrogeology and Hydrochemistry laboratory of UNESP's Department of Applied Geology and at the Chemistry School of the National University (Heredia, Costa Rica). All results were expressed in per mil relative to Vienna Standard Mean Ocean Water (V-SMOW). The certified calibration standards used in UNESP were USGS-45 (δ^2H = −10.3‰, $\delta^{18}O$ = −2.24‰), USGS-46 (δ^2H = −236.0‰, $\delta^{18}O$ = −29.80‰), including one internal standard (Cachoeira de Emas - CE – δ^2H = −36.1‰, $\delta^{18}O$ = −5.36‰). USGS standards were used to calibrate the results on the V-SMOW2-SLAP2 scale, whereas CE was used for memory and drift corrections. In Costa Rica laboratory, the certified standards MTW (δ^2H = −130.3‰, $\delta^{18}O$ = −16.7‰), USGS45 (δ^2H = −10.3‰, $\delta^{18}O$ = −2.2‰), and CAS (δ^2H = −64.3‰, $\delta^{18}O$ = −8.3‰) were used to correct the measurement results for memory and drift effects and to calibrate them on the V-SMOW2-SLAP2 scale (García-Santos et al., 2022). The analytical uncertainty was ±1.2‰ (1σ) for δ^2H and ±0.2‰ (1σ) for $\delta^{18}O$ for UNESP analysis and 0.07‰ $\delta^{18}O$ and 0.38‰ δ^2H for Costa Rica analysis. Deuterium excess (*d*-excess) was calculated as: *d*-excess = $\delta^2H - 8*\delta^{18}O$ (Dansgaard, 1964). It was used to interpret the influence of moisture origin/transport (Sánchez-Murillo et al., 2017; Froehlich et al., 2002) and to quantify below-cloud processes (e.g. Jeelani et al., 2018; Graf et al., 2019; Aemisegger et al., 2015b).

2.3 Meteorological data

Automatic Weather Station (AWS) Decagon Em50 (METER) was installed near the Micro Rain Radar (MRR) (METEK) at 670 m.a.s.l, in immediate vicinity of the rainfall collection site. Meteorological data were recorded at 1 min intervals for rain rate (AWS RR, $mm.min^{-1}$), air temperature (T, °C), relative humidity (RH, %) and pressure (kPa). The MRR data for reflectivity (Z, dBZ), fall velocity (w, $m.s^{-1}$), liquid water content (LWC, $g.m^{-3}$) and rain rate (MRR RR, $mm.min^{-1}$) were also recorded at 1 min intervals. MRR parameters correspond to the mean values measured at the elevation between 150 and 350 meters above ground. MRR operated at a frequency of 24.230 GHz, modulation of 0.5 – 15 MHz according to the height resolution. For this work, different height resolutions (31 range bin) were tested, 150m, 200m, 300m and 350m, resulting in vertical profiles of 4650m, 6200m, 9300m and 10.850m, respectively (Endries et al., 2018). The MRR data used in the following discussion are the near-surface data (first measurement from 150m to 350m). MRR vertical profile (from 150m to 10.850m) was used to classify and visualize the radar echoes. Rain rates (AWS and MRR) were computed for 5 min intervals ($mm.5min^{-1}$) following the chosen interval of isotope rainfall sampling. Lifting Condensation Level (LCL, meters) was computed from AWS RH and T, following Soderberg et al. (2013).

GOES-16 imagery (https://home.chpc.utah.edu/~u0553130/Brian_Blaylock/cgi-bin/goes16_download.cgi) was used to identify the convective nuclei of the cloud-top (10.35-μm, Band-13) and brightness temperature (BT), at 10 min intervals during the sampling period over the Rio Claro station (Ribeiro et al., 2019; Schmit et al., 2017). The 10.35-μm BT is often

https://doi.org/10.5194/egusphere-2023-710
Preprint. Discussion started: 15 May 2023

used to estimate the convective cloud depth, since the lower BT is linked to deeper cloud tops (Adler and Fenn, 1979; Roberts and Rutledge, 2003; Adler and Mack, 1986; Ribeiro et al., 2019; Machado et al., 1998).

The origin of air masses and moisture transport (Fig. 1e) were analysed using the HYSPLIT Model (Stein et al., 2015; Soderberg et al., 2013). Trajectories of convective events were estimated for t 240 hours prior to rainfall collection and ending elevations at 1500m above the surface, following (dos Santos et al., (2022). The meteorological outputs: heights (meters), relative humidity (%), and rainfall intensity ($mm.hr^{-1}$) along the trajectories were used to analyse the rainout processes.

Reanalysis data were used to better understand the influence of atmospheric circulation on isotopic composition of rainfall at the study area. ERA-5 climatology (https://cds.climate.copernicus.eu/cdsapp#!/search?type=dataset) was used to generate plots of hourly vertical integral of eastward water vapor flux during convective events sampled. The Global Modelling and Assimilation Office (GMAO) data (MERRA-2, 1 hour, 0.5 x 0.625 degree, V5.12.4 - https://goldsmr4.gesdisc.eosdis.nasa.gov/data/MERRA2/M2T1NXFLX.5.12.4/) were used calculations of latent heat flux (LHF), and Aqua/AIRS L3 Daily Standard Physical Retrieval (AIRS-only) 1 degree x 1 degree V7.0, Greenbelt, MD, USA, Goddard Earth Sciences Data and Information Services Center (GES DISC) data, for average outgoing longwave radiation (OLR) (https://disc.gsfc.nasa.gov/datasets/AIRS3STD_7.0/summary). OLR values below $240W.m^{-2}$ indicate organized deep convection (Gadgil, 2003).

2.4 Convective rainfall classification

In General, classification of convective precipitation systems was based on the vertical structure of precipitation (lack of the melting layer and bright band - BB) in the radar profiles featuring high reflectivity values (Z >38 dBZ) (Houze, 1993, 1997; Steiner and Smith, 1998; Rao et al., 2008; Mehta et al., 2020; Endries et al., 2018) and satellite imagery (Vila et al., 2008; Ribeiro et al., 2019; Siqueira et al., 2005; Machado et al., 1998). Consequently, convective rainfall was defined in this study by (i) convective nuclei observed in GOES-16 imagery, (ii) no BB detected, (iii) Z > 38dBZ near-surface and (iv) rainfall intensity (AWS) of at least $10mm.h^{-1}$ (Klaassen, 1988) (Fig. 1c,d). The convective nuclei were identified using GOES-16 imagery, determined as a contiguous area of at least 40 pixels with BT lower than 235K (≤-38°C) over Rio Claro station, according to previous studies (Ribeiro et al., 2019).

2.5 Definition of day-night differences in convective rainfall

The rainfall samples collected in this study generally do not represent consecutive pairs of day-night data during the same day. Daytime data are related to rainfall samples collected in Rio Claro station from 07:00 to 18:59 local time (10:00-21:59 UTC) whereas night-time data represent the period 19:00-06:59 local time (22:00-09:59 UTC). Therefore, the labelling of convective rainfall samples as ‘day’ or ‘night’ is directly related to the period of their collection at the Rio Claro station. It was not the focus of this study to evaluate the formation of convection processes and evolution of a convective system, because we only

https://doi.org/10.5194/egusphere-2023-710
Preprint. Discussion started: 15 May 2023

collected rainfall samples in a single point. An evaluation of the evolution of convection during the day-night using high-frequency strategies would require a range of collection stations capable of capturing the formation of the convective system and its spatial and temporal evolution. Although, in the tropics, a substantial part of the convection systems is developed during the day (Warner et al., 2003; Romatschke and Houze, 2010), they can generate rain events in the afternoon and at night, not occurring in the same place. Proper sampling of these systems, following their formation, development, and decay would require a complex and expensive sampling strategy.

2.6 Statistical tests

The Shapiro-Wilk test was applied to verify that the data distribution was normal (parametric) or non-normal (non-parametric) (Shapiro and Wilk, 1965). A significant difference (p-value < 0.05) indicates a non-parametric distribution. A Spearman rank correlation test was used for nonparametric data distribution, whereas Pearson's linear correlation test was applied for parametric data. A Kruskal-Wallis nonparametric test (Kruskal and Wallis, 1952) was applied to test statistical differences (p-value < 0.05) between the isotopic compositions ($\delta^{18}O$ and *d*-excess) for day-night during summer, and between autumn and spring. All tests were performed with significance levels defined by a p-value (p) < 0.05, using R statistical package (R Core Team, 2022).

3 Results

3.1 Seasonal variations of rainfall isotopes and meteorological parameters

The high-frequency sampling allowed a more detailed and robust analysis of rainfall formation processes and its isotope characteristics as compared to previous studies in the region (dos Santos et al., 2022; Dos Santos et al., 2019), which were based on monthly or daily composite rainfall samples. Figure 2a illustrate this monthly perspective of isotope characteristics ($\delta^{18}O$ and *d*-excess) of rainfall for the study period (September 2019 – February 2021) at the Rio Claro site. It reveals a sharp seasonal isotopic contrast between rainy and dry season (austral summer and winter, respectively). The Local Meteoric Water Lines (LMWL) for the Rio Claro site based on monthly cumulative and high-frequency samples (Fig. A1 -Appendix A) cannot be directly compared because of not complete coverage of rainfall in the given month by the high-frequency sampling. The high-frequency sampling strategy employed in the study was aimed to capture specific rainfall events for each season (cf. Fig. 2a).

The seasonal and day-night distributions of convective activity (Fig. 2b,c) and rainfall amount (Fig. 2d) were observed during the study period, resulting in different conditions for occurrence of convective events and high-frequency sampling of rainfall. In austral winter, a season characterized by dry conditions in the south-central tropics of Brazil, convective rainfall events were largely absent (Fig. 2a). No rainfall was collected at night during spring (convective events occurred predominantly during day hours). Covid-19 restrictions precluded rainfall collection at night. Contrary to summer months, during autumn,

https://doi.org/10.5194/egusphere-2023-710
Preprint. Discussion started: 15 May 2023

spring and winter latent heat fluxes were lower (Fig. 2b) and outgoing longwave radiation was larger (Fig. 2c), which in turn may have inhibited convective development related to thermal forcings (Houze, 1997, 1989). During summer, strong diurnal heating and persisting convective activity resulted in nearly equal total rainfall amounts during day (51%) and night (49%) (Fig. 2d).

3.2 Day-night differences in meteorological parameters and isotopic characteristics of convective rainfall.

Strong day-night variations in the isotopic parameters $\delta^{18}O$, d-excess of convective rainfall were observed during the austral summer (red box-plots in Fig. 3). Day and night median $\delta^{18}O$ values were equal -7.5‰ and -13.0‰, respectively. During daytime, higher $\delta^{18}O$ values (-4.4‰ ~ -11.6‰, Fig. 3a), lower *d*-excess values (1.2‰ ~ 18.4‰, median 8.4‰ - Fig. 3d), lower AWS rain rates (median 1.0mm·5min^{-1} – Fig. 3g) and AWS rainfall amount (median 16.9 mm) were observed. In contrast, lower $\delta^{18}O$ values (-7.9‰ ~ -15.2‰), higher *d*-excess (4.8‰ ~ 21.4‰, median 16.7‰), higher AWS rain rates (median 1.8mm·5min^{-1}) and AWS rainfall amount (median 26.9 mm) were observed night-time convective events. The non-parametric Kruskal-Wallis test shows significant differences between day and night isotopic composition (p=<0.0001 for $\delta^{18}O$ and *d*-excess).

Similar $\delta^{18}O$ values (Fig. 3b,c) were observed in autumn (median -3.1‰) and spring (median -3.2‰), while *d*-excess values (Fig. 3e,f) and AWS rain rates (Fig. 3h,i) differ between both seasons, (autumn: 16.8‰ and 0.6mm·5min^{-1}; spring: 22.2‰ and 1.2mm·5min^{-1}) (Fig. 3e,f). The Kruskal-Wallis test shows significant differences between autumn and spring and for the *d*-excess (p=0.0039) and AWS rain rates (p=0.04), except $\delta^{18}O$ (p=0.36).

Differences in convective rainfall between seasons were also observed in the origin of moisture tracked back by HYSPLIT modelling (Fig. 1e), accompanied by differences in median $\delta^{18}O$ and *d*-excess values (in parentheses below, respectively) (Fig. 3 color-coded). In summer, convective events during daytime exhibited trajectories from Amazon (-10.4‰ and 13.4‰) and Southwest (-6.7‰ and 7.1‰), and predominantly from Amazon at night-time (-13.0‰ and 16.7‰). The Atlantic Ocean moisture source was dominant during autumn (-3.3‰ and 17.2‰ for daytime, -2.8‰ and 16.2‰, night-time) and spring (-3.1‰ and 22.9‰), but also mixing with more isotopically depleted moisture of the Amazon origin (-4.1‰ and 19.7‰) was suggested by HYSPLIT simulations for few events.

Figure 4 illustrates different meteorological scenarios for isotope parameters ($\delta^{18}O$ and *d*-excess). During summer, in daytime higher $\delta^{18}O$ and lower *d*-excess values correspond to low relative humidity values (RH) (Fig. 4a), high lifting condensation level – (LCL) (Fig. 4f) and low brightness temperature – (BT) (Fig. 4k). At night-time, slightly lower $\delta^{18}O$ values and higher *d*-excess correspond to higher RH (Fig. 4b), lower LCL (Fig. 4g) and higher BT values (Fig. 4l). For these variables strong and significant ($p < 0.05$) correlations were observed (Table 1): during daytime $\delta^{18}O$-RH (r = -0.51), $\delta^{18}O$-T (r = -0.64), $\delta^{18}O$-AWS rain rate (r = -0.57), *d*-excess and AWS rain rate (r 0.61), *d*-excess and Z (r 0.61), *d*-excess and MRR rain rate (r

https://doi.org/10.5194/egusphere-2023-710
Preprint. Discussion started: 15 May 2023

0.61) and night-time δ^{18}O-RH (r = -0.74), *d*-excess and RH (r = 0.51,), δ^{18}O-LCL (r = 0.75), *d*-excess and LCL (r -0.52), δ^{18}O-T (r = 0.50).

During autumn and spring, the isotopic composition of convective rainfall is influenced by frontal systems (Fig. 4r,s,t) (Dos Santos et al., 2019) which are characterized by (i) the passage of a cold front over the study area, (ii) instability (frontal), when a cold front is localized in the south of Brazil and it generates changes in the regional atmosphere over São Paulo, and (iii) when the cold front is localized in the Atlantic Ocean near Southeast portion of Brazil and interacts with regional atmosphere, generating a low pressure (frontal). In summer, frontal systems and frontal instabilities occurred during the daytime (Fig. 4p), while instability (thermal) and low pressure were present only at night (Fig. 4q). The instability (thermal) is the atmospheric ascend related to surface heat in inland Brazil, mainly during summer.

Slightly higher median meteorological values were observed in spring when compared to autumn, except for LCL (449m autumn-night and 225m spring), RH (AWS, 95% autumn-day and 93% spring) and RH (HYSPLIT, 78% autumn-day, 73 autumn-night and 41% spring) (Table B1). Also, the relations between rainfall isotopic composition and meteorological parameters are not very clear in these seasons (Fig. 3). In general, correlations between isotope ratios and meteorological variables in spring and in autumn are rather weak (Table 1), except for δ^{18}O-BT during autumn (r = 0.53).

3.3 Conceptual model of convective rainfall during summer

A conceptual model of the observed day/night isotopic variability of convective rainfall at the Rio Claro site is presented in Fig. 5. The measured meteorological variables help us to better characterize the convective cloud/rainfall during passage over the sampling site, the local atmosphere-surface conditions, and their impact on the observed isotope signatures of rainfall. BT and LCL are related to the convective cloud depth (Machado and Laurent, 2004; Ribeiro et al., 2019) and cloud base (Risi et al., 2019; Hu et al., 2022), respectively. RH and rainfall rates (from MRR and from AWS) indicate atmospheric conditions below the cloud base and at the surface (Graf et al., 2019; Aemisegger et al., 2015a).

For daytime conditions, median values of meteorological and isotope parameters suggest strong convective cloud depth and elevated cloud base (lower BT and high LCL values), the later resulting in longer interaction time between raindrops the ambient atmosphere below the cloud base level. Lower RH enhances partial evaporation of raindrops, decreasing median value of rainfall rate (both MRR and AWS readings), and producing less negative δ^{18}O and lower *d*-excess values. During night-time, less vigorous convective cloud depth (higher BT) and low cloud base level (low LCL) were observed, which resulted in reduced time of interaction raindrops with the atmosphere below the cloud base. High RH at the surface combined with higher median rainfall intensity, further reduced the extend of raindrops evaporation. Consequently, stable isotope signatures generated during in-cloud processes were transferred without substantial changes to the samples of rainfall collected at the ground.

https://doi.org/10.5194/egusphere-2023-710
Preprint. Discussion started: 15 May 2023

4 Discussion

We are not directly interpreting the convection processes (not include vapor isotopes data), but rather the consequence of this mechanism reflected in rainwater. For this reason, our dataset represents case studies of rain events over our collection point (Fig. 1), whose classification was based mainly on point vertical radar observation, agreed with Houze (1997), that the convective adjective must be used to describe the precipitation (or radar echo) and convection (or convective activity) is a dynamic concept, the rapid, efficient, vigorous overturning of the atmosphere, directly related to the formation of clouds in the tropics (Houze, 1997, 1993).

Isotopic composition of convective rainfall is a function of two main factors: (i) rainout history of moist air masses during their transport in the atmosphere, from the source region(s) to the collection site, and (ii) local effects associated with convective cloud characteristics at a given location linked to the fractionation steps associated with in-cloud phase changes of water such as vapour-to-liquid and/or, vapour-to-solid, and modifications of rainfall isotopic composition below the cloud-base level due to partial evaporation of raindrops as well as isotope exchange with the ambient moisture.

Regional aspects of atmospheric moisture transport to the Rio Claro site are illustrated in Fig. 1e showing representative HYSPLIT backward trajectories associated with convective rainfall whereas maps of vertically integrated moisture flux in the region are shown in Fig. 6. During summer, most of the moisture supply to the rainfall collection site is associated with northwest-southeast winds bringing moisture from the Amazon basin. Moist air masses of Atlantic origin are transported westward over the Amazon Forest, undergoing intensive recycling and rainout. Strong topographic blocking effect of the Andes induces a change in the wind direction to northwest-southeast, along the eastern slope of the Andes, allowing flow of moisture from the Amazon Basin to the southeast of Brazil (Fig. 6a) (Marengo et al., 2004; Vera et al., 2006). Along this pathway, the occurrence of regional convective activity (Fig. 6d) generates successive convective systems resulting in continuous rainout (Fig. A2) and vapour recycling (Moerman et al., 2013; Risi et al., 2008; Vimeux et al., 2011), which leads to the characteristic depletion of convective rainfall in heavy isotope contents ($\delta^{18}O$ around -10‰). Intensive convective activity during summer results in large amounts of rainfall reaching the land surface during this season (Fig. A2).

In contrast to summer rainy season when moist, rain-producing air masses arriving at Rio Claro station are predominantly of the Amazon origin, during autumn and spring the rainfall is associated exclusively with Atlantic Ocean and/or Amazon, respectively. These air masses and largely suppressed convective activity during autumn (Fig. 6e) and spring (Fig. 6f) generate convective systems with lower continuous rainout (Fig. A2) and vapor recycling. Very high $\delta^{18}O$ values, with median equal -3.1‰ (autumn) and -3.2‰ (spring), accompanied by high *d*-excess values (median equal ca. 16.8 and 22.2‰, respectively (cf. Fig.2), can be explained only by two processes: (i) first–step condensation of water vapour of marine origin (Atlantic Ocean), and/or (ii) first step condensation of evapotranspirated moisture of continental origin which has the isotopic composition of regional rainfall in the study area, stored in the soil during the rainy season ($\delta^{18}O$ equal ca. -10 per mil). HYSPLIT modelling suggests further that, during spring, two types of moist air masses are contributing to the characterize differences in isotopic composition of convective rainfall: (i) continental air masses arriving from the Amazon, and (ii)

https://doi.org/10.5194/egusphere-2023-710
Preprint. Discussion started: 15 May 2023

maritime air masses arriving from the Atlantic Ocean. It is apparent from Fig. 3b,c that these two types of air masses reveal slightly different isotope signatures: median $\delta^{18}O$ correspond to -4.1‰ and -3.1‰, respectively, with *d*-excess values substantially lower for continental moist air masses when compared to maritime air masses (19.7‰ and 22.9‰, respectively) (Fig. 3e,f). It is apparent from Fig. 1e, that backward trajectories starting at the Atlantic Ocean may interact also with the continent (mixing with re-evaporated water vapour and partial rainout over the continent) before they reach the Rio Claro site. This is supported by slightly reduced $\delta^{18}O$ and elevated *d*-excess values observed when compared to rainfall events of purely continental origin.

The high-frequency of rainfall sampling implemented in this study revealed yet another dimension of the isotopic variability of summer rainfall in the tropics: day versus night time differences in convective rainfall (cf. Fig. 3a,d). The night-time rainfall is depleted in heavy isotopes and has elevated *d*-excess values, when compared to the daytime rainfall. During summer rainy season in the southwest of Brazil is under overwhelming influence of moist air masses arriving from the Amazon basin. Night-time rainfall events were predominantly from Amazon air masses. The occurrence of night-time events was limited and likely linked to the occurrence of the low-level jet during the night (Saulo et al., 2000; Nicolini et al., 2002). These air masses have a long history which could be linked to long residence time of water vapor in the atmosphere, in the order of 10 days (Gimeno et al., 2010). This in turn, combined with rainout and moisture recycling, may lead to distinct depletion in heavy isotope contents and elevated *d*-excess values of the moisture precipitating over the Rio Claro site. Therefore, it is highly unlikely that the sharp day-night contrast in the isotope characteristics of convective rainfall shown in Fig. 3a,d is generated by only moist air masses of different origin. Instead, we suggest that those strong diurnal variations of the isotopic composition of convective rainfall in the inland tropics of Brazil are mainly controlled by local effects.

Impact of local processes on the isotopic composition of convective rainfall in the tropics is illustrated by the conceptual model presented in Fig. 5. This diagram combines (a) meteorological parameters characterizing the convective cloud structure (cloud-top temperature and cloud-base level) and rainfall interactions with the local atmosphere below the cloud-base level (ground-level relative humidity, lifting condensation level, raindrops dimensions and rainfall rate) with (b) the processes modifying the isotopic composition of raindrops below the cloud-base level (partial evaporation and isotope exchange with ambient moisture). We suggest that night-time isotopic composition of convective rainfall largely reflects regional conditions characterized by presence of moist air masses of Amazon origin depleted in heavy isotopes and having elevated *d*-excess values, with the LLJ playing a relevant role in the moisture transport from the Amazon to the collection site area. It is suggested that partial evaporation and isotope exchange of raindrops below the cloud-base level seems to be suppressed at night due to number of factors such as: (i) shorter travel time of raindrops to the ground due to both lower cloud-base level and higher terminal velocity of large raindrops formed during night-time events, (ii) smaller relative mass reduction of large raindrops leading to smaller modification of their isotopic composition due to partial evaporation, (iii) higher RH of the ambient atmosphere below the cloud-base level reducing intensity of raindrops evaporation. These factors change during daytime, resulting in a substantial modification of the original isotopic composition of raindrops leaving the cloud base (longer travel time of raindrops, higher relative mass reduction of raindrops, lower RH of ambient atmosphere below the cloud-base level).

https://doi.org/10.5194/egusphere-2023-710
Preprint. Discussion started: 15 May 2023

Our conceptual model supports previous studies related to possible factors modifying the isotopic composition of precipitation below the cloud base level such as drop size distribution (Muller et al., 2015; Managave et al., 2016), below-cloud RH (Lee and Fung, 2008), height of the cloud base (Wang et al., 2016) and rain intensity (Graf et al., 2019). However, it is mentioned that a more detailed assessment of precipitation evaporation below the cloud base must be conducted and include further details of the vertical profiles of temperature and humidity as well as water vapor isotopes information if possible.

Absence of day-night isotope contrasts of rainfall during the autumn and spring seasons (cf. Fig. 2) is probably related to lower surface heating and hence lower possibility of convection to generate convective rainfall by thermal conditions (cf. Fig. 6e,f). Apparently, generally weaker convection activity of the regional atmosphere during this period does not generate day-night differences in the extent and intensity of rain-producing convective systems, large enough to induce discernible difference in the isotopic characteristics of rainfall.

5 Concluding remarks

This work provides a new perspective on the isotopic variability of convective rainfall in the tropics. We combined high-frequency sampling of rainfall, covering a 1.5-year period (September 2019 – February 2021), with extensive monitoring of meteorological parameters in the local atmosphere, satellite imagery and HYSPLIT backward trajectory modelling of moist air masses bringing rainfall the Rio Claro site, a continental, tropical location in the south-eastern Brazil.

On monthly time scale, the Rio Claro site reveals typical variability observed in other tropical sites, with high amount of rainfall during the rainy period, strongly depleted in heavy isotopes, and high δ values during the dry period. High-frequency, intra-event sampling implemented in this work revealed an unexpected characteristic of the sampled convective rainfall fractions. A distinct diurnal variability was discovered, with large differences in the δ values and the *d*-excess parameter between the daytime and night-time rainfall fractions. A conceptual model, based on local high-frequency meteorological observations, satellite imagery and HYSPLIT modelling was proposed to explain the observed diurnal variations of the isotopic composition of the collected rainfall fractions. We suggest that the observed diurnal variability is largely caused by local effects, i.e. the differences in the convective clouds structure, rain-producing systems during daytime and night-time causing large changes in the isotope signatures of daytime rainfall due to partial evaporation of raindrops below the cloud-base level and apparent absence of those effects for night-time rainfall fractions.

Day-night differences and diurnal cycle in water isotopic composition of convective systems presented here offers an interesting new perspective for the ongoing discussion of the ‘amount effect’ in tropical areas.

Although high-frequency rainfall sampling is logistically difficult, we encourage future studies of this type in different geographical regions across the tropics, to search for diurnal variations in the isotopic composition of convective rainfall during rainy period. Such studies should be accompanied by extensive monitoring of local meteorological parameters and modelling of regional transport of moisture to the rainfall collection site.

https://doi.org/10.5194/egusphere-2023-710
Preprint. Discussion started: 15 May 2023

Financial support

This work was funded by grants the São Paulo Research Foundation (FAPESP) under Processes 2018/06666-4, 2019/03467-3 and 2021/10538-4, and by the International Atomic Energy Agency Grant CRP-F31006.

Acknowledgment

FAPESP support for the scholarship provided under the Process 2019/03467-3 and 2021/10538-4 is acknowledged. Durán-Quesada acknowledges time for analysis and writing provided within UCR C1038 project.

References

Adler, R. F. and Fenn, D. D.: Thunderstorm Vertical Velocities Estimated from Satellite Data, American, 36, 1747–1754, https://doi.org/10.1175/1520-0469(1979)036,1747: TVVEFS.2.0.CO;2., 1979.

Adler, R. F. and Mack, R. A.: Thunderstorm Cloud Top Dynamics as Inferred from Satellite Observations and a Cloud Top Parcel Model, American Meteorological Society, 43, 1945–1960, https://doi.org/10.1175/ 1520-0469(1986)043,1945:TCTDAI.2.0.CO;2, 1986.

Aemisegger, F., Spiegel, J. K., Pfahl, S., Sodemann, H., Eugster, W., and Wernli, H.: Isotope meteorology of cold front passages: A case study combining observations and modeling, Geophysical Research Letters, 42, 5652–5660, https://doi.org/10.1002/2015GL063988, 2015a.

Aemisegger, F. ., Spiegel, J. K. ., Pfahl, S. ., Sodemann, H. ., Eugster, W. ., and Wernli, H.: Isotope meteorology of cold front passages: A case study combining observations and modeling, Geophysical Research Letters, 42, 5652–5660, https://doi.org/10.1002/2015GL063988, 2015b.

Aggarwal, P. K., Romatschke, U., Araguas-Araguas, L., Belachew, D., Longstaffe, F. J., Berg, P., Schumacher, C., and Funk, A.: Proportions of convective and stratiform precipitation revealed in water isotope ratios, Nature Geoscience, 9, 624–629, https://doi.org/10.1038/ngeo2739, 2016.

Celle-Jeanton, H., Gonfiantini, R., Travi, Y., and Sol, B.: Oxygen-18 variations of rainwater during precipitation: Application of the Rayleigh model to selected rainfalls in Southern France, Journal of Hydrology, 289, 165–177, https://doi.org/10.1016/j.jhydrol.2003.11.017, 2004.

Coplen, T. B., Neiman, P. J., White, A. B., Landwehr, J. M., Ralph, F. M., and Dettinger, M. D.: Extreme changes in stable hydrogen isotopes and precipitation characteristics in a landfalling Pacific storm, Geophysical Research Letters, 35, L21808, https://doi.org/10.1029/2008GL035481, 2008.

Dansgaard, W.: Stable isotopes in precipitation, Tellus, 16, 436–468, https://doi.org/10.3402/tellusa.v16i4.8993, 1964.

Donat, M. G., Alexander, L. V., Yang, H., Durre, I., Vose, R., Dunn, R. J. H., Willett, K. M., Aguilar, E., Brunet, M., Caesar, J., Hewitson, B., Jack, C., Klein Tank, A. M. G., Kruger, A. C., Marengo, J., Peterson, T. C., Renom, M., Oria Rojas, C., Rusticucci, M., Salinger, J., Elrayah, A. S., Sekele, S. S., Srivastava, A. K., Trewin, B., Villarroel, C., Vincent, L. A., Zhai,

https://doi.org/10.5194/egusphere-2023-710
Preprint. Discussion started: 15 May 2023

P., Zhang, X., and Kitching, S.: Updated analyses of temperature and precipitation extreme indices since the beginning of the twentieth century: The HadEX2 dataset, Journal of Geophysical Research Atmospheres, 118, 2098–2118, https://doi.org/10.1002/jgrd.50150, 2013.

Endries, J. L., Perry, L. B., Yuter, S. E., Seimon, A., Andrade-Flores, M., Winkelmann, R., Quispe, N., Rado, M., Montoya, N., Velarde, F., and Arias, S.: Radar-observed characteristics of precipitation in the tropical high andes of Southern Peru and Bolivia, Journal of Applied Meteorology and Climatology, 57, 1441–1458, https://doi.org/10.1175/JAMC-D-17-0248.1, 2018.

Froehlich, K., Gibson, J. J., and Aggarwal, P.: Deuterium excess in precipitation and its climatological significance, Journal of Geophysical Research-Atmospheres, 1–23, 2002.

Gadgil, S.: The Indian monsoon and its variability, Annual Review of Earth and Planetary Sciences, 31, 429–467, https://doi.org/10.1146/annurev.earth.31.100901.141251, 2003.

García-Santos, S., Sánchez-Murillo, R., Peña-Paz, T., Chirinos-Escobar, M. J., Hernández-Ortiz, J. O., Mejía-Escobar, E. J., and Ortega, L.: Water stable isotopes reveal a complex rainfall to groundwater connectivity in central Honduras, Science of the Total Environment, 844, https://doi.org/10.1016/j.scitotenv.2022.156941, 2022.

Garreaud, R. D.: Cold air incursions over subtropical South America: Mean structure and dynamics, Monthly Weather Review, 128, 2544–2559, https://doi.org/10.1175/1520-0493(2000)128<2544:caioss>2.0.co;2, 2000.

Gimeno, L., Drumond, A., Nieto, R., Trigo, R. M., and Stohl, A.: On the origin of continental precipitation, Geophysical Research Letters, 37, 1–7, https://doi.org/10.1029/2010GL043712, 2010.

Graf, P., Wernli, H., Pfahl, S., and Sodemann, H.: A new interpretative framework for below-cloud effects on stable water isotopes in vapour and rain, Atmospheric Chemistry and Physics, 19, 747–765, https://doi.org/10.5194/acp-19-747-2019, 2019.

Han, X., Lang, Y., Wang, T., Liu, C.-Q., Li, F., Wang, F., Guo, Q., Li, S., Liu, M., Wang, Y., and Xu, A.: Temporal and spatial variations in stable isotopic compositions of precipitation during the typhoon Lekima (2019), China, Science of The Total Environment, 762, 143143, https://doi.org/10.1016/j.scitotenv.2020.143143, 2021.

Houze, R.: Stratiform precipitation in regions of convection: A Meteorological Paradox?, Bulletin of the American Meteorological Society, 78, 2179–2195, 1997.

Houze, R. A.: Cloud dynamics, Academic Press Limited, 573 pp., https://doi.org/10.1016/0377-0265(87)90017-0, 1993.

Houze, R. A. J.: Observed structure of mesoscale convective systems and implications for large-scale heating., Quart. J. Roy. Meteor. Soc., 115, 425–461, 1989.

Hu, J., Emile-Geay, J., Nusbaumer, J., and Noone, D.: Impact of Convective Activity on Precipitation δ18O in Isotope-Enabled General Circulation Models, Journal of Geophysical Research: Atmospheres, 123, 13,595-13,610, https://doi.org/10.1029/2018JD029187, 2018.

Hu, J., Bailey, A., Nusbaumer, J., Dee, S., Sasser, C., and Worden, J.: Tracking Shallow Convective Mixing and Its Influence on Low-Level Clouds With Stable Water Isotopes in Vapor, Journal of Geophysical Research: Atmospheres, 127,

https://doi.org/10.5194/egusphere-2023-710
Preprint. Discussion started: 15 May 2023

https://doi.org/10.1029/2021JD035355, 2022.

IPCC, W. G. I.-T. P. S. B.: Regional fact sheet – Central and South America, Sixth Assessment Report, 1–2 pp., 2021.

Jeelani, G., Deshpande, R. D., Galkowski, M., and Rozanski, K.: Isotopic composition of daily precipitation along the southern foothills of the Himalayas: Impact of marine and continental sources of atmospheric moisture, Atmospheric Chemistry and Physics, 18, 8789–8805, https://doi.org/10.5194/acp-18-8789-2018, 2018.

Klaassen, W.: Radar Observations and Simulation of the Melting Layer of Precipitation, Journal of the Atmospheric Sciences, 45, 3741–3753, 1988.

Kodama, Y.: Large-scale common features of subtropical precipitation zones (the Baiu Frontal Zone , the SPCZ , and the SACZ) Part I: Characteristics of subtropical frontal zones, Journal of the Meteorological Society of Japan, 70, 813–836, https://doi.org/10.1248/cpb.37.3229, 1992.

Kruskal, W. H. and Wallis, W. A.: Use of Ranks in One-Criterion Variance Analysis, Journal of the American Statistical Association, 47, 583–621, 1952.

Kurita, N.: Water isotopic variability in response to mesoscale convective system over the tropical ocean, Journal of Geophysical Research Atmospheres, 118, 10376–10390, https://doi.org/10.1002/jgrd.50754, 2013a.

Kurita, N.: Water isotopic variability in response to mesoscale convective system over the tropical ocean, Journal of Geophysical Research Atmospheres, 118, 10,376-10,390, https://doi.org/10.1002/jgrd.50754, 2013b.

Lawrence, J. R., Gedzelman, S. D., Dexheimer, D., Cho, H. K., Carrie, G. D., Gasparini, R., Anderson, C. R., Bowman, K. P., and Biggerstaff, M. I.: Stable isotopic composition of water vapor in the tropics, Journal of Geophysical Research-Atmospheres, 109, 16, https://doi.org/D0611510.1029/2003jd004046, 2004.

Lee, J. and Fung, I.: "Amount effect" of water isotopes and quantitative analysis of post-condensation processes, Hydrological Processes, 22, 1–8, https://doi.org/10.1002/hyp.6637, 2008.

Lekshmy, P. R., Midhun, M., Ramesh, R., and Jani, R. A.: 18 O depletion in monsoon rain relates to large scale organized convection rather than the amount of rainfall, Scientific Reports, 4, 1–5, https://doi.org/10.1038/srep05661, 2014.

Luiz Silva, W., Xavier, L. N. R., Maceira, M. E. P., and Rotunno, O. C.: Climatological and hydrological patterns and verified trends in precipitation and streamflow in the basins of Brazilian hydroelectric plants, Theoretical and Applied Climatology, 137, 353–371, https://doi.org/10.1007/s00704-018-2600-8, 2019.

Machado, L. A. T. and Laurent, H.: The convective system area expansion over Amazonia and its relationships with convective system life duration and high-level wind divergence, Monthly Weather Review, 132, 714–725, https://doi.org/10.1175/1520-0493(2004)132<0714:TCSAEO>2.0.CO;2, 2004.

Machado, L. A. T. and Rossow, W. B.: Structural Characteristics and Radiative Properties of Tropical Cloud Clusters, Monthly Weather Review, 121, 3234–3260, 1993.

Machado, L. A. T., Rossow, W. B., Guedes, R. L., and Walker, A. W.: Life cycle variations of mesoscale convective systems over the Americas, Monthly Weather Review, 126, 1630–1654, https://doi.org/10.1175/1520-0493(1998)126<1630:LCVOMC>2.0.CO;2, 1998.

https://doi.org/10.5194/egusphere-2023-710
Preprint. Discussion started: 15 May 2023

Managave, S. R., Jani, R. A., Narayana Rao, T., Sunilkumar, K., Satheeshkumar, S., and Ramesh, R.: Intra-event isotope and raindrop size data of tropical rain reveal effects concealed by event averaged data, Climate Dynamics, 47, 981–987, https://doi.org/10.1007/s00382-015-2884-7, 2016.

Marengo, J. A., Soares, W. R., Saulo, C., and Nicolini, M.: Climatology of the low-level jet east of the Andes as derived from the NCEP-NCAR reanalyses: Characteristics and temporal variability, Journal of Climate, 17, 2261–2280, https://doi.org/10.1175/1520-0442(2004)017<2261:COTLJE>2.0.CO;2, 2004.

Marengo, J. A., Ambrizzi, T., Alves, L. M., Barreto, N. J. C., Simões Reboita, M., and Ramos, A. M.: Changing Trends in Rainfall Extremes in the Metropolitan Area of São Paulo: Causes and Impacts, Frontiers in Climate, 2, 1–13, https://doi.org/10.3389/fclim.2020.00003, 2020.

Mehta, S., Mehta, S. K., Singh, S., Mitra, A., Ghosh, S. K., and Raha, S.: Characteristics of the Z–R Relationships Observed Using Micro Rain Radar (MRR-2) over Darjeeling (27.05° N, 88.26° E): A Complex Terrain Region in the Eastern Himalayas, Pure and Applied Geophysics, 177, 4521–4534, https://doi.org/10.1007/s00024-020-02472-6, 2020.

Moerman, J. W., Cobb, K. M., Adkins, J. F., Sodemann, H., Clark, B., and Tuen, A. A.: Diurnal to interannual rainfall δ18O variations in northern Borneo driven by regional hydrology, Earth and Planetary Science Letters, 369–370, 108–119, https://doi.org/10.1016/j.epsl.2013.03.014, 2013.

Muller, C. L., Baker, A., Fairchild, I. J., Kidd, C., and Boomer, I.: Intra-Event Trends in Stable Isotopes: Exploring Midlatitude Precipitation Using a Vertically Pointing Micro Rain Radar, Journal of Hydrometeorology, 16, 194–213, https://doi.org/10.1175/JHM-D-14-0038.1, 2015.

Munksgaard, N. C., Zwart, C., Haig, J., Cernusak, L. A., and Bird, M. I.: Coupled rainfall and water vapour stable isotope time series reveal tropical atmospheric processes on multiple timescales, Hydrological Processes, 34, 111–124, https://doi.org/10.1002/hyp.13576, 2020.

Nicolini, M., Saulo, A. C., Torres, J. C., and Salio, P.: Enhanced Precipitation Over Southeastern South America Related To Strong Low-Level Jet Events During Austral Warm Season, Meteorologica, 27, 59–69, 2002.

R Core Team: A language and environment for statistical computing. R Foundation for Statistical Computing, Vienna, Austria. https://www.R-project.org/., 2022.

Rao, N. T., Kirankumar, N. V. P., Radhakrishna, B., and Rao, N. D.: Classification of tropical precipitating systems using wind profiler spectral moments. Part I: Algorithm description and validation, Journal of Atmospheric and Oceanic Technology, 25, 884–897, https://doi.org/10.1175/2007JTECHA1031.1, 2008.

Ribeiro, B. Z., Machado, L. A. T., Biscaro, T. S., Freitas, E. D., Mozer, K. W., and Goodman, S. J.: An evaluation of the GOES-16 rapid scan for nowcasting in southeastern brazil: Analysis of a severe hailstorm case, Weather and Forecasting, 34, 1829–1848, https://doi.org/10.1175/WAF-D-19-0070.1, 2019.

Risi, C., Bony, S., Vimeux, F., Descroix, L., Ibrahim, B., Lebreton, E., Mamadou, I., and Sultan, B.: What controls the isotopic composition of the African monsoon precipitation? Insights from event-based precipitation collected during the 2006 AMMA field campaign, Geophysical Research Letters, 35, 1–6, https://doi.org/10.1029/2008GL035920, 2008.

https://doi.org/10.5194/egusphere-2023-710
Preprint. Discussion started: 15 May 2023

Risi, C., Galewsky, J., Reverdin, G., and Brient, F.: Controls on the water vapor isotopic composition near the surface of tropical oceans and role of boundary layer mixing processes, 20, 1–37, 2019.

Roberts, R. D. and Rutledge, S.: Nowcasting storm initiation and growth using GOES-8 and WSR-88D data, Weather and Forecasting, 18, 562–584, https://doi.org/10.1175/1520-0434(2003)018<0562:NSIAGU>2.0.CO;2, 2003.

Romatschke, U. and Houze, R. A.: Extreme summer convection in South America, Journal of Climate, 23, 3761–3791, https://doi.org/10.1175/2010JCLI3465.1, 2010.

Romatschke, U. and Houze, R. A.: Characteristics of precipitating convective systems accounting for the summer rainfall of tropical and subtropical South America, Journal of Hydrometeorology, 14, 25–46, https://doi.org/10.1175/JHM-D-12-060.1, 2013.

Rozanski, K., Sonntag, C., and Munnich, K. O.: Factors controlling stable isotope composition of European precipitation., Tellus, 34, 142–150, https://doi.org/10.3402/tellusa.v34i2.10796, 1982.

Rozanski, K., Araguás-Araguás, L., and Gonfiantini, R.: Isotopic Patterns in Modern Global Precipitation, 1–36, https://doi.org/10.1029/GM078p0001, 1993.

Sánchez-Murillo, R., Durán-Quesada, A. M., Birkel, C., Esquivel-Hernández, G., and Boll, J.: Tropical precipitation anomalies and d-excess evolution during El Niño 2014-16, Hydrological Processes, 31, 956–967, https://doi.org/10.1002/hyp.11088, 2017.

Sánchez-Murillo, R., Durán-Quesada, A. M., Esquivel-Hernández, G., Rojas-Cantillano, D., Birkel, C., Welsh, K., Sánchez-Llull, M., Alonso-Hernández, C. M., Tetzlaff, D., Soulsby, C., Boll, J., Kurita, N., and Cobb, K. M.: Deciphering key processes controlling rainfall isotopic variability during extreme tropical cyclones, Nature Communications, 10, 1–10, https://doi.org/10.1038/s41467-019-12062-3, 2019.

Dos Santos, V. ., Gastmans, D. ., Sánchez-Murillo, R. ., Gozzo, L. F. ., Batista, L. V. ., Manzione, R. L. ., and Martinez, J.: Regional atmospheric dynamics govern interannual and seasonal stable isotope composition in southeastern Brazil, Journal of Hydrology, 579, 124136, https://doi.org/10.1016/j.jhydrol.2019.124136, 2019.

dos Santos, V., Marshall Fleming, P., Henrique Mancini, L., Dalva Santos Cota, S., de Lima, G. B., Rodrigues Gomes, R., Kirchheim, R. E., Sanchéz-Murillo, R., and Gastmans, D.: Distinguishing the Regional Atmospheric Controls on Precipitation Isotopic Variability in the Central-Southeast Portion of Brazil, Advances in Atmospheric Sciences, 39, 1693–1708, https://doi.org/10.1007/s00376-022-1367-0, 2022.

Saulo, a. C., Nicolini, M., and Chou, S. C.: Model characterization of the South American low-level flow during the 1997-1998 spring-summer season, Climate Dynamics, 16, 867–881, https://doi.org/10.1007/s003820000085, 2000.

Schmit, T. J., Griffith, P., Gunshor, M. M., Daniels, J. M., Goodman, S. J., and Lebair, W. J.: A closer look at the ABI on the goes-r series, Bulletin of the American Meteorological Society, 98, 681–698, https://doi.org/10.1175/BAMS-D-15-00230.1, 2017.

Schumacher, C. and Houze, R. A.: Stratiform rain in the tropics as seen by the TRMM precipitation radar, Journal of Climate, 16, 1739–1756, https://doi.org/10.1175/1520-0442(2003)016<1739:SRITTA>2.0.CO;2, 2003.

https://doi.org/10.5194/egusphere-2023-710
Preprint. Discussion started: 15 May 2023

Shapiro, S. S.; Wilk, M. B.: An analysis of variance test for normality (complete samples), Biometrika, 53, 591–611, 1965.

Siqueira, J. R., Rossow, W. B., Machado, L. A. T., and Pearl, C.: Structural characteristics of convective systems over South America related to cold-frontal incursions, Monthly Weather Review, 133, 1045–1064, https://doi.org/10.1175/MWR2888.1, 2005.

Soderberg, K., Good, S. P., O'connor, M., Wang, L., Ryan, K., and Caylor, K. K.: Using atmospheric trajectories to model the isotopic composition of rainfall in central Kenya, Ecosphere, 4, 1–18, https://doi.org/10.1890/ES12-00160.1, 2013.

Stein, A. F., Draxler, R. R., Rolph, G. D., Stunder, B. J. B., Cohen, M. D., and Ngan, F.: Noaa's hysplit atmospheric transport and dispersion modeling system, Bulletin of the American Meteorological Society, 96, 2059–2077, https://doi.org/10.1175/BAMS-D-14-00110.1, 2015.

Steiner, M. and Smith, J. A.: Convective versus stratiform rainfall: An ice-microphysical and kinematic conceptual model, Atmospheric Research, 47–48, 317–326, https://doi.org/10.1016/S0169-8095(97)00086-0, 1998.

Sun, C., Shanahan, T. M., and Partin, J.: Controls on the Isotopic Composition of Precipitation in the South-Central United States, Journal of Geophysical Research: Atmospheres, 124, 8320–8335, https://doi.org/10.1029/2018JD029306, 2019.

Sun, C., Tian, L., Shanahan, T. M., Partin, J. W., Gao, Y., Piatrunia, N., and Banner, J.: Isotopic variability in tropical cyclone precipitation is controlled by Rayleigh distillation and cloud microphysics, Communications Earth & Environment, 3, https://doi.org/10.1038/s43247-022-00381-1, 2022.

Tharammal, T., G. Bala, and D. N.: Impact of deep convection on the isotopic amount effect in tropical precipitation, Journal of Geophysical Research Atmospheres, 122, 1505–1523, https://doi.org/10.1002/2016JD025555, 2017.

Vera, C., Baez, J., Douglas, M., Emmanuel, C. B., Marengo, J., Meitin, J., Nicolini, M., Nogues-Paegle, J., Paegle, J., Penalba, O., Salio, P., Saulo, C., Silva Dias, M. A., Silva Dias, P., and Zipser, E.: The South American low-level jet experiment, Bulletin of the American Meteorological Society, 87, 63–77, https://doi.org/10.1175/BAMS-87-1-63, 2006.

Vila, D. A., Machado, L. A. T., Laurent, H., and Velasco, I.: Forecast and tracking the evolution of cloud clusters (ForTraCC) using satellite infrared imagery: Methodology and validation, Weather and Forecasting, 23, 233–245, https://doi.org/10.1175/2007WAF2006121.1, 2008.

Vimeux, F., Tremoy, G., Risi, C., and Gallaire, R.: A strong control of the South American SeeSaw on the intra-seasonal variability of the isotopic composition of precipitation in the Bolivian Andes, Earth and Planetary Science Letters, 307, 47–58, https://doi.org/10.1016/j.epsl.2011.04.031, 2011.

Vuille, M., Bradley, R. S., Werner, M., Healy, R., and Keimig, F.: Modeling δ18O in precipitation over the tropical Americas: 1. Interannual variability and climatic controls, Journal of Geophysical Research: Atmospheres, 108, 1–24, https://doi.org/10.1029/2001JD002038, 2003.

Wang, S., Zhang, M., Che, Y., Zhu, X., and Liu, X.: Influence of below-cloud evaporation on deuterium excess in precipitation of arid Central Asia and its meteorological controls, Journal of Hydrometeorology, 17, 1973–1984, https://doi.org/10.1175/JHM-D-15-0203.1, 2016.

Wang, T. and Tang, G.: Spatial Variability and Linkage Between Extreme Convections and Extreme Precipitation Revealed

https://doi.org/10.5194/egusphere-2023-710
Preprint. Discussion started: 15 May 2023

by 22-Year Space-Borne Precipitation Radar Data, Geophysical Research Letters, 47, 1–10, https://doi.org/10.1029/2020GL088437, 2020.

Warner, T. T., Mapes, B. E., and Xu, M.: Diurnal patterns of rainfall in northwestern South America. Part II: Model simulations, Monthly Weather Review, 131, 813–829, https://doi.org/10.1175/1520-0493(2003)131<0813:DPORIN>2.0.CO;2, 2003.

Winnick, M. J., Chamberlain, C. P., Caves, J. K., and Welker, J. M.: Quantifying the isotopic "continental effect," Earth and Planetary Science Letters, 406, 123–133, https://doi.org/10.1016/j.epsl.2014.09.005, 2014.

Worden, J., Noone, D., Bowman, K., Beer, R., Eldering, A., Fisher, B., Gunson, M., Goldman, A., Herman, R., Kulawik, S. S., Lampel, M., Osterman, G., Rinsland, C., Rodgers, C., Sander, S., Shephard, M., Webster, C. R., and Worden, H.: Importance of rain evaporation and continental convection in the tropical water cycle, Nature, 445, 528–532, https://doi.org/10.1038/nature05508, 2007.

World Meteorological Organization: WMO Atlas of Mortality and Economic Losses From Weather , Climate and Water Extremes, 2019.

Zilli, M. T., Carvalho, L. M. V., Liebmann, B., and Silva Dias, M. A.: A comprehensive analysis of trends in extreme precipitation over southeastern coast of Brazil, International Journal of Climatology, 37, 2269–2279, https://doi.org/10.1002/joc.4840, 2017.

Zwart, C., Munksgaard, N. C., Lambrinidis, D., Bird, M. I., Protat, A., and Kurita, N.: The isotopic signature of monsoon conditions , cloud modes , and rainfall type, Hydrological Processes, 2296–2303, https://doi.org/10.1002/hyp.13140, 2018.

https://doi.org/10.5194/egusphere-2023-710
Preprint. Discussion started: 15 May 2023

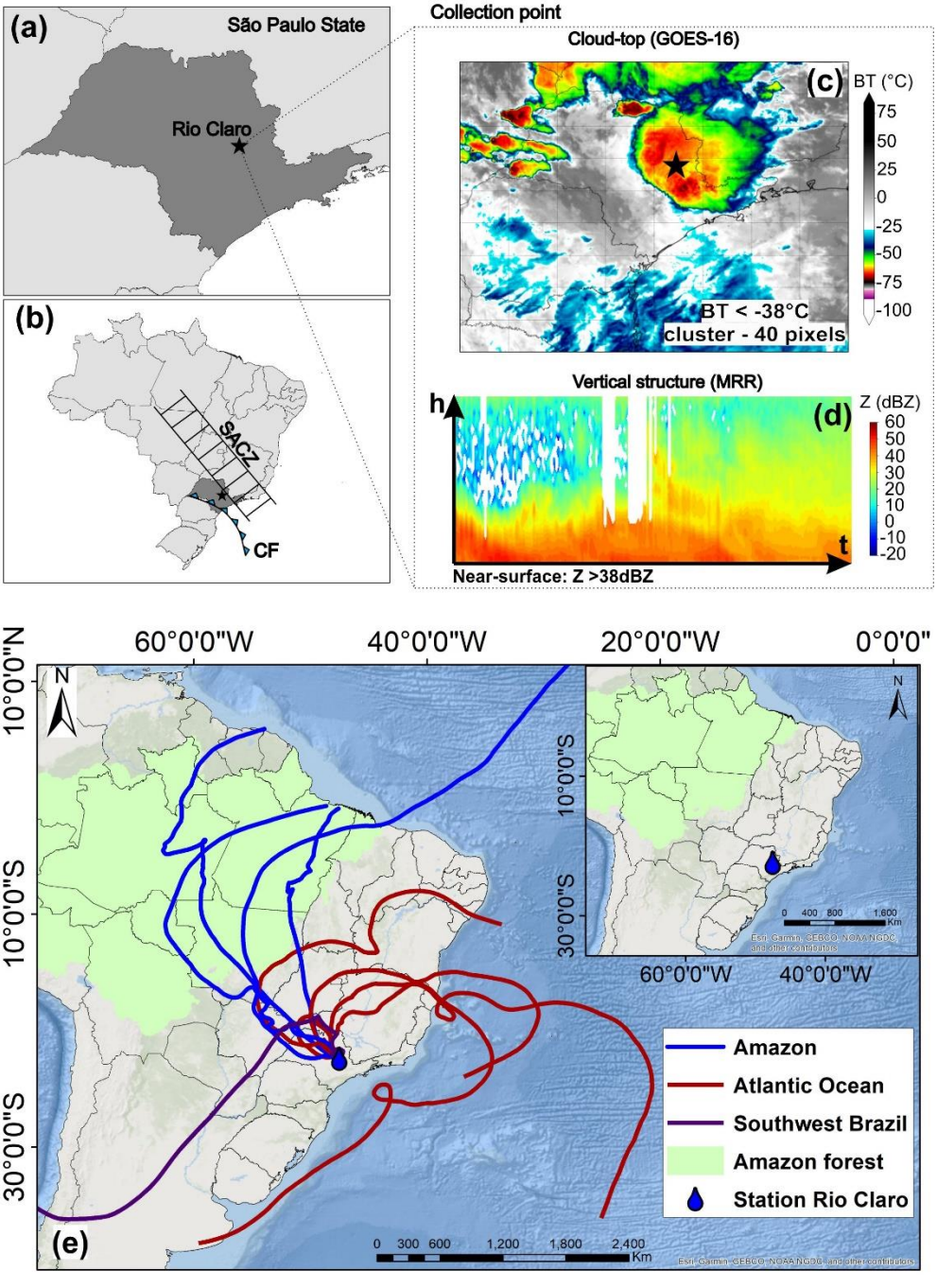

Figure 1. (a) Localization of sampling site in Rio Claro (black star) (b) in regional synoptic context across Brazil and main atmospheric systems (CF – cold front and SACZ – Southern Atlantic Convergence Zone). Over collection point (c) GOES-16 satellite imagery showed convective system with lower brightness temperature (BT, clou-top) and (d) Micro Rain Radar (MRR) illustrates the vertical structure of convective rainfall, height (h) and time (t), characterized by radar reflectivity (Z) with strong values near-surface. (e) transport of atmospheric moisture to the site visualized by air mass back trajectories derived from HYSPLIT modelling. In Figure 1e, the authors used trivial information, the borders of the countries and the ocean provided by the ESRI base map.

https://doi.org/10.5194/egusphere-2023-710
Preprint. Discussion started: 15 May 2023

575

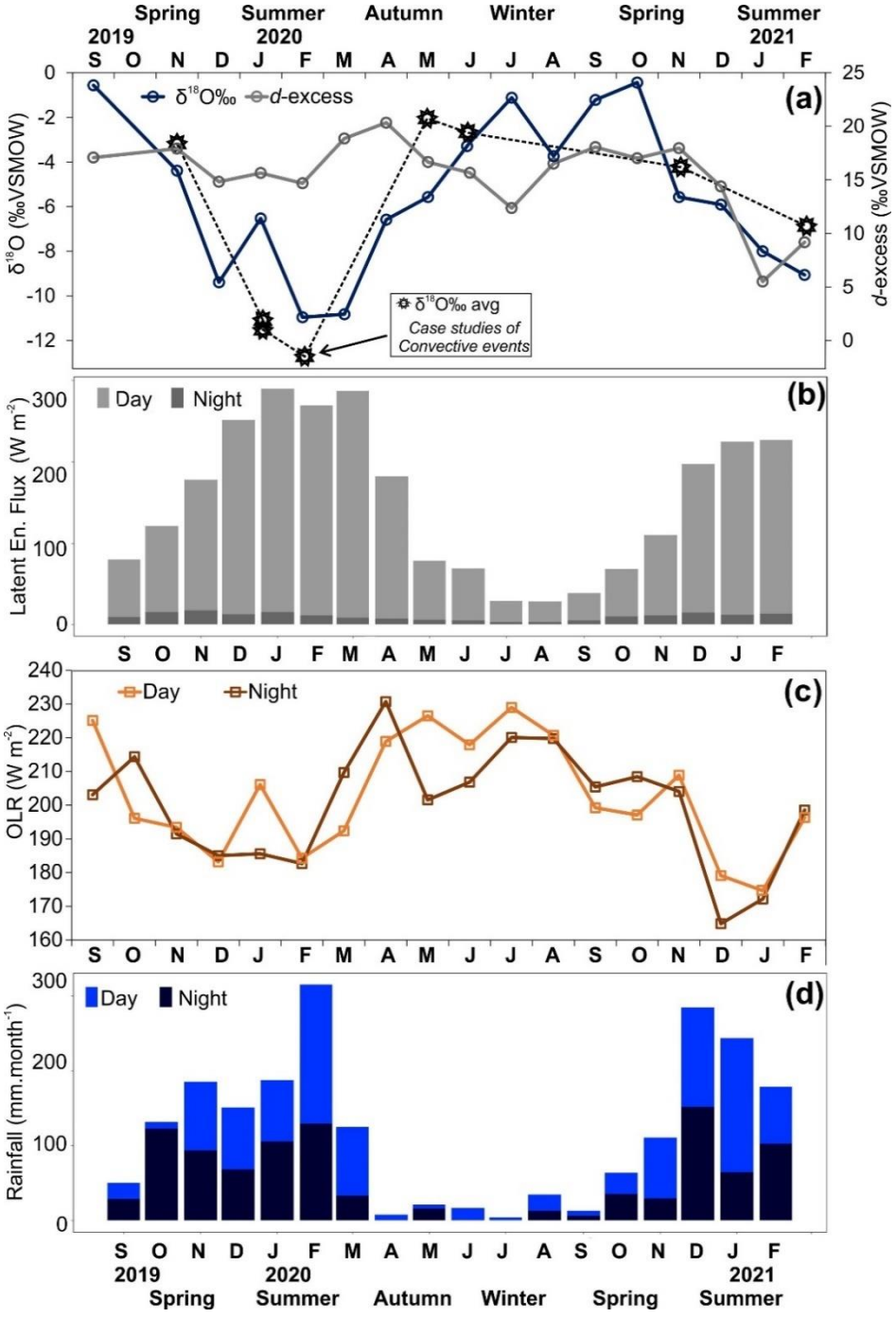

Figure 2. (a) Seasonal variation of $\delta^{18}O$ and *d*-excess values in monthly rainfall and aggregated monthly $\delta^{18}O$ values high-frequency convective rainfall sampling discussed in this study (b) AQUA/AIRS latent heat flux. (c) MERRA-2 outgoing longwave radiation (monthly averaged daytime and night-time data) (d) monthly rainfall amounts at Rio Claro separated into day and night fraction (no rainfall types distinguished).

580

https://doi.org/10.5194/egusphere-2023-710
Preprint. Discussion started: 15 May 2023

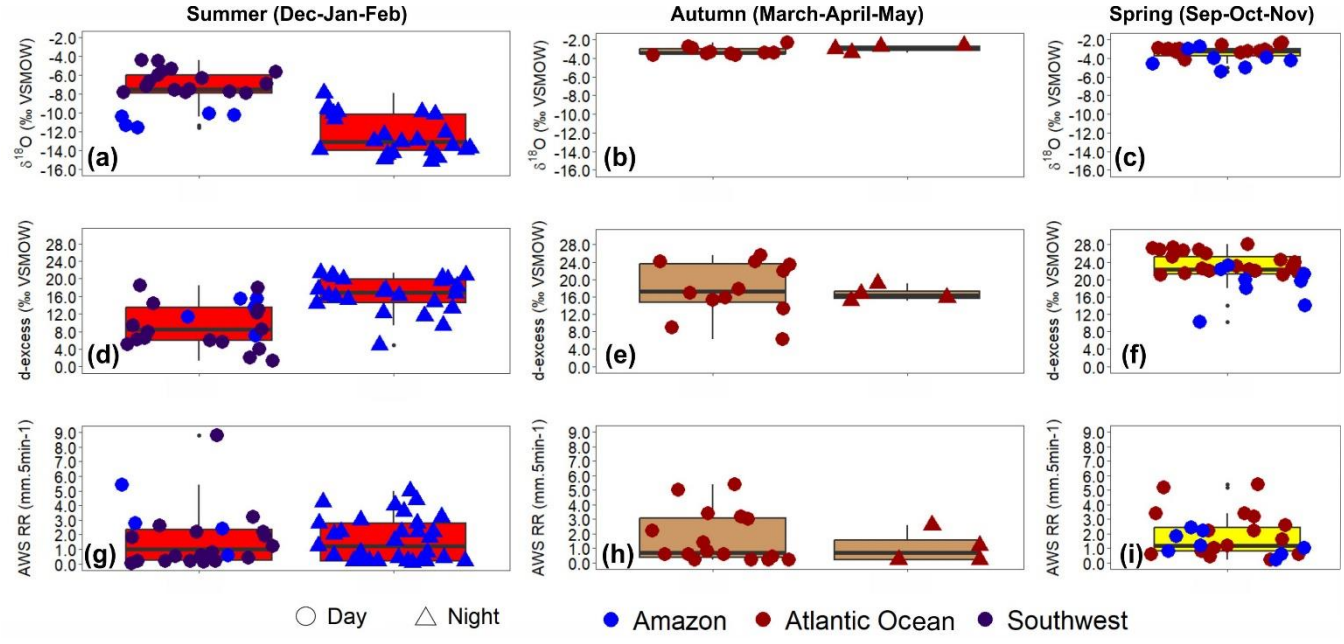

Figure 3. (a, b, c) $\delta^{18}O$, (d, e, f) *d*-excess and (g, h, i) AWS rainfall rates in seasonal color-coded box-plots for summer (red), autumn (light brown) and spring (yellow), during day (circle) and night (triangle) time. Symbols are color-coded by the HYSPLIT derived origin of rain-producing air masses based on Fig. 1e: Amazon (blue), Atlantic Ocean (reddish purple) and Southwest Brazil (dark purple). Summer is defined as the period from December to February, autumn from March to April and spring from September to November.

https://doi.org/10.5194/egusphere-2023-710
Preprint. Discussion started: 15 May 2023

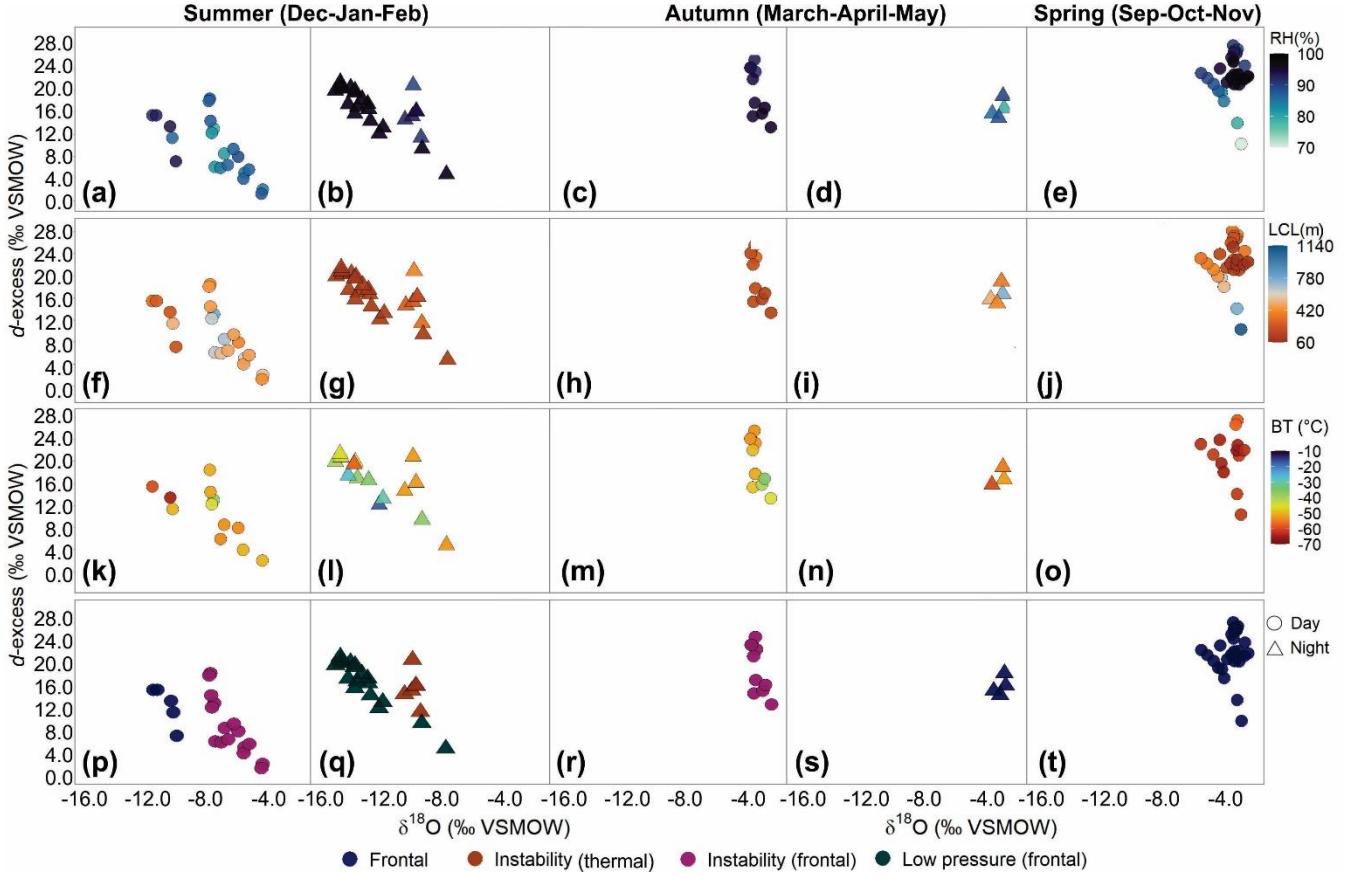

Figure 4. (a, b, c) AWS RH, (d, e, f) LCL – lifting condensation level (meters), (g, h, i) GOES-16 BT – brightness temperature and (j, k, l) atmospheric systems with *d*-excess and $\delta^{18}O$ at daytime (circle) and night-time (triangle) for summer, autumn and spring seasons.

https://doi.org/10.5194/egusphere-2023-710
Preprint. Discussion started: 15 May 2023

Table 1. Spearman rank correlations between isotopic composition of rainfall and meteorological parameters

Seasons		**Summer**				**Autumn***		**Spring**	
		Day		**Night**					
Isotopes		$\delta^{18}O$	*d*-excess	$\delta^{18}O$	*d*-excess	$\delta^{18}O$	*d*-excess	$\delta^{18}O$	*d*-excess
GOES	BT	0.43	-0.08	-0.25	-0.19	**0.53**	-0.08	0.14	-0.26
MRR	Z	-0.38	**-0.19**	-0.14	0.32	0.34	-0.29	**-0.22**	0.55
	w	**-0.16**	**-0.26**	-0.14	0.10	0.14	-0.19	**-0.13**	0.59
	LWC	-0.07	**-0.35**	-0.20	0.41	0.00	-0.11	**-0.29**	0.45
	RR	**-0.52**	**-0.22**	**-0.40**	**0.37**	0.00	0.00	**-0.25**	0.36
AWS	LCL	**0.47**	**0.75**	**0.86**	**-0.68**	**-0.33**	**0.40**	**-0.42**	-0.16
	Temp	**-0.64**	**0.5**	-0.22	0.11	-0.56	0.56	0.48	0.4
	RH	**-0.51**	**-0.74**	**-0.86**	**0.68**	**0.30**	**-0.38**	**0.42**	0.16
	RR	**-0.57**	-0.19	**-0.34**	**0.41**	**0.16**	0.00	**-0.18**	0.11

Bold values are significant (p-value <0.05**).** BT (°C) - GOES brightness temperature; MRR - Micro Rain Radar; Z (dBZ)- reflectivity; w ($m \cdot s^{-1}$)- vertical velocity; LWC ($g \cdot m^{-3}$) - liquid water content; RR (mm) - rain rate; AWS - Automatic Weather Station; LCL (meters) - lifting condensation level; T (°C) - temperature; RH (%) - relative humidity; RR (mm) - rain rate. *****For autumn the correlations were not separated into day and night, because the number of samples representing night is very small (n=4).

https://doi.org/10.5194/egusphere-2023-710
Preprint. Discussion started: 15 May 2023

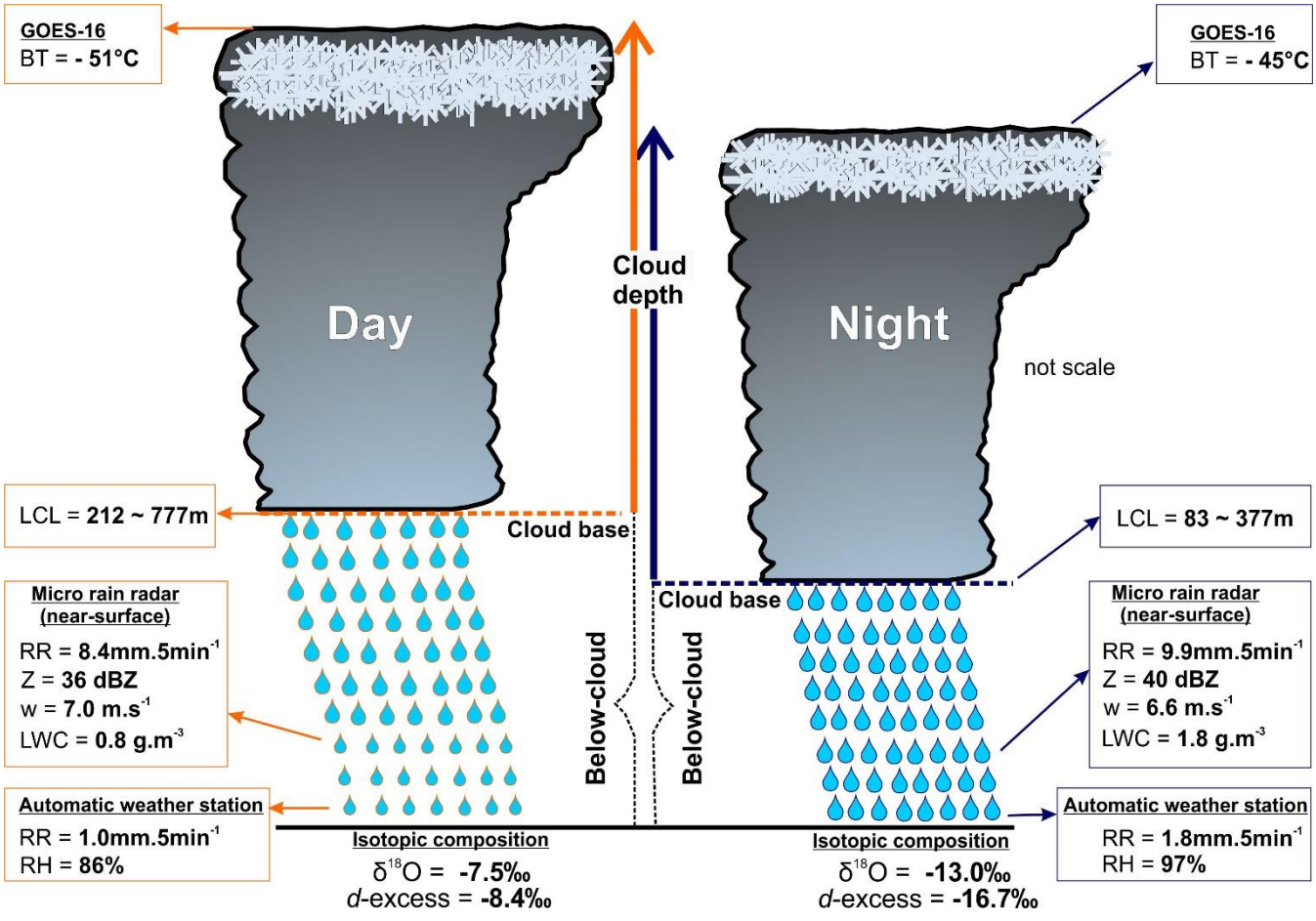

Figure 5. Schematic diagram for daytime (orange) and night-time (dark-blue) situations of convective rainfall occurrences during summer at the inland tropics of Brazil. Vertical structure of convective cloud is characterized by the cloud depth (GOES-16 BT – brightness temperature °C) and cloud-base (LCL – lifting condensation levels in meters). Below-cloud illustrate falling raindrops and their interactions with atmosphere near-surface (150m-350m) by Micro rain radar data, RR – rain rates, Z – reflectivity, w – fall velocity, LWC – liquid water content and at surface by Automatic weather station, RR – rain rates, ΔT - difference between maximum and minimum surface air temperature and RH – relative humidity. Differences in cloud structure and atmosphere below-cloud generate the differences in isotopic composition ($\delta^{18}O$ and *d*-excess) of convective rainfall observed. The illustration of cloud and raindrops are not scale.

https://doi.org/10.5194/egusphere-2023-710
Preprint. Discussion started: 15 May 2023

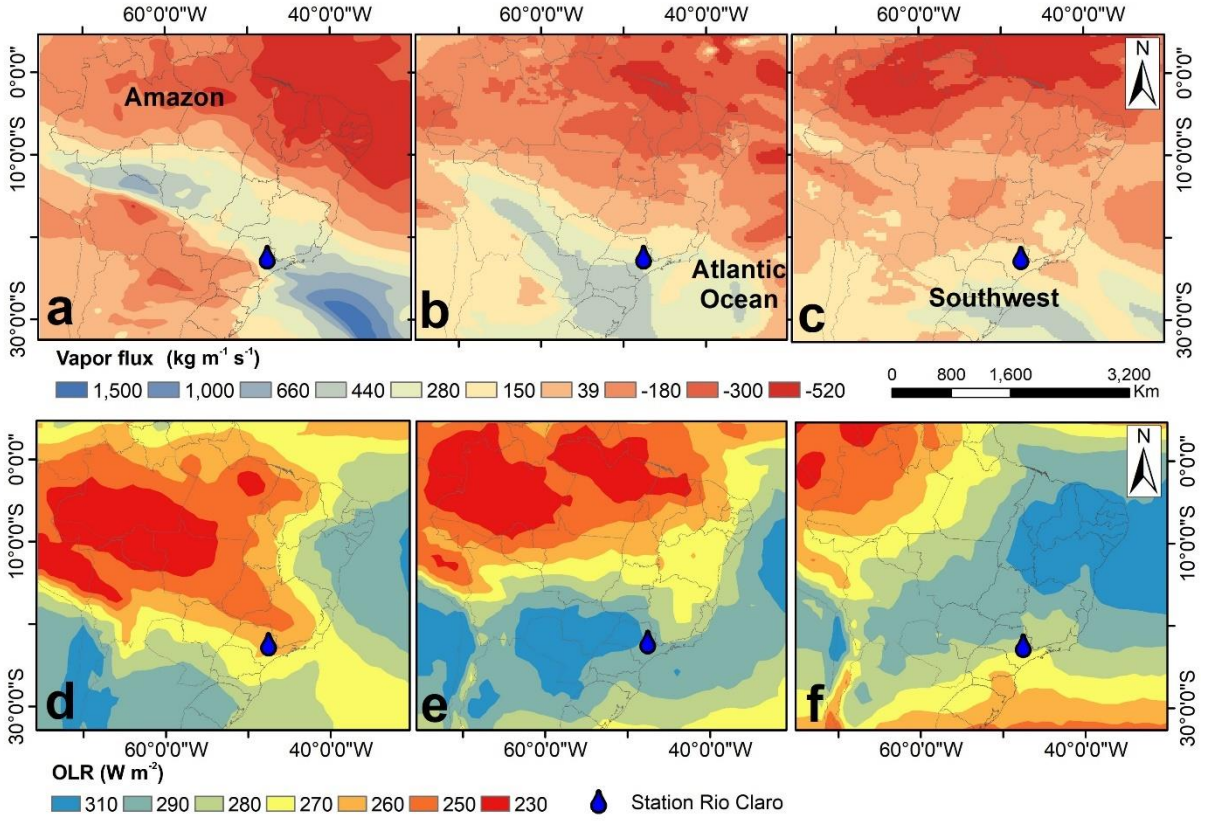

Figure 6. (a) Amazon, (b) Atlantic Ocean and (c) Southwest Brazil are HYSPLIT origin and were combined with ERA-5 vertical integral of eastward water vapor flux for the days when convective rainfall events occurred, during (d) summer, (e) autumn and (f) spring aggregated with MERRA-2 outgoing longwave radiation between 2019 and 2021. The position of the names indicates the origin of HYSPLIT trajectories. Positive values in Fig. a,b,c indicate the direction of moisture vapor flux from left to right, and negative values from right to left. Lower OLR (red) values indicate higher convective activity.

https://doi.org/10.5194/egusphere-2023-710
Preprint. Discussion started: 15 May 2023

Appendices

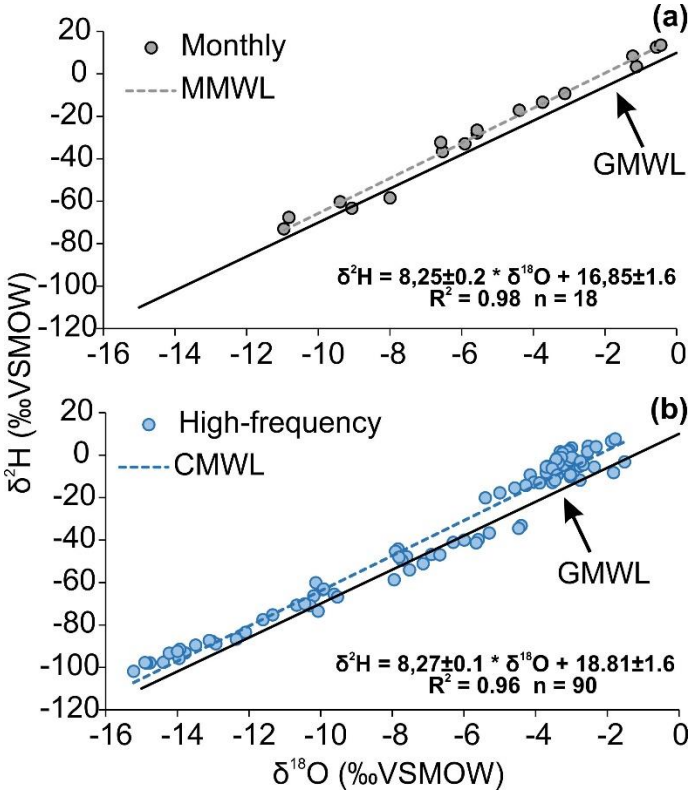

Figure A1. (a) Monthly and (b) high-frequency δ^2H and $\delta^{18}O$ rainfall data plotted in the $\delta^2H/\delta^{18}O$ space. LMWL – local meteoric water line based on monthly values, CMWL – convective meteoric water line and GMWL – global meteoric water line.

https://doi.org/10.5194/egusphere-2023-710
Preprint. Discussion started: 15 May 2023

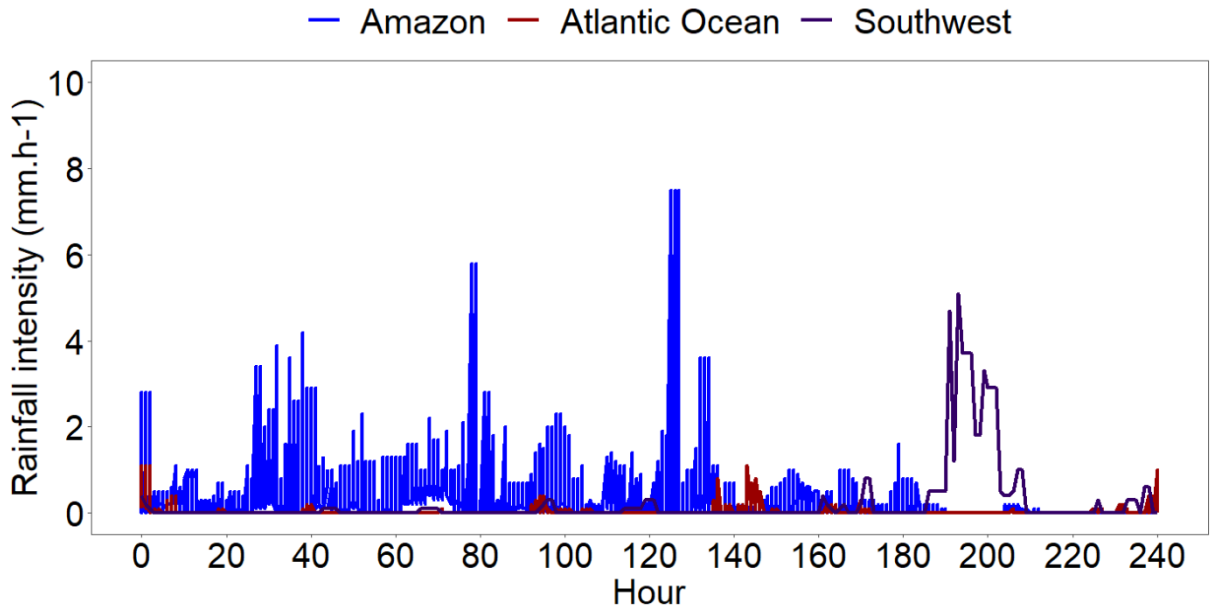

Figure A2. Rainfall intensity on HYSPLIT backward trajectories (240 hours) related to the moisture origin (Figure 1e) for all convective events. The Amazon trajectories reveal quasi-continuous rainout during pathway of moist air masses over the Amazon Basin down to the collection site at Rio Claro.

https://doi.org/10.5194/egusphere-2023-710
Preprint. Discussion started: 15 May 2023

Table B1. Meteorological data for summer (day and night), autumn (day and night) and spring (day)

Seasons		**Summer**						**Autumn**						**Spring**		
Meteorological data		**Daytime**			**Night-time**			**Daytime**			**Night-time**					
		min	max	**median**	min	max	**median**	min	max	**median**	min	max	**median**	min	max	**median**
GOES	BT	-66	-39	**-51**	-57.8	-16.2	**-45**	-55	-36	**-50**	-61	-53	**-56**	-66.7	-57.3	**-63**
MRR	Z	20	51	**36**	0.93	46	**40**	17	51	**42**	22	44	**33**	24	50	**45**
	w	5.4	8.8	**7.0**	0.26	7.7	**6.6**	5.6	8.7	**7.6**	5.0	8.1	**6.6**	5.4	8.9	**7.8**
	LWC	0.0	14.0	**0.8**	0.03	7.6	**1.8**	0.1	3.8	**1.2**	0.1	3.3	**1.0**	0.0	4.0	**2.1**
	RR	0.5	10.0	**8.4**	0.27	10.0	**9.9**	0.02	10	**8.9**	5.0	8.1	**6.6**	1.0	10	**9**
AWS	LCL	212	777	**452**	83	377	**95**	133	340	**167**	355	757	**449**	65	1137	**225**
	Temp	19	25	**21**	20	24	**22**	18	20	**19**	18	20	**19**	19	27	**21**
	RH	79	94	**86**	89	98	**97**	90	96	**95**	78	89	**86**	71	98	**93**
	RR	0.03	8.8	**1.0**	0.1	5.0	**1.8**	0.01	5.4	**0.6**	0.2	2.6	**0.7**	0.2	5.4	**1.2**
HYSPLIT	Height	31	1110	**1727**	0	3212	**778**	1185	3576	**2030**	44	1500	**287**	0	11104	**1781**
	RH	2	100	**71**	32	100	**78**	42	90	**78**	54	92	**73**	2	100	**41**
	Rainfall	0.00	10.70	**0.37**	0.00	13.20	**0.53**	0.00	1.00	**0.01**	0.00	1.10	**0.01**	0.00	2.40	**0.03**

Bolded values were used to create the figure 5. BT (°C) - GOES brightness temperature; MRR - Micro Rain Radar; Z (dBZ)- reflectivity; w ($m \cdot s^{-1}$)- vertical velocity; LWC ($g \cdot m^{-3}$) - liquid water content; RR ($mm.5min^{-1}$) – rain rate; AWS - Automatic Weather Station; LCL (meters) - lifting condensation level; T (°C) - temperature; RH (%) - relative humidity; RR ($mm.5min^{-1}$) – rain rate. Meteorological values along HYSPLIT trajectories; (meters) height; RH (%) - relative humidity; Rainfall rate ($mm.h^{-1}$).